nature microbiology

ARTICLES

https://doi.org/10.1038/s41564-020-0704-2

Yeasts collectively extend the limits of habitable temperatures by secreting glutathione

Diederik S. Laman Trip[1,2] and Hyun Youk[1,2,3]✉

The conventional view is that high temperatures cause microorganisms to replicate slowly or die. In this view, microorganisms autonomously combat heat-induced damages. However, microorganisms co-exist with each other, which raises the underexplored and timely question of whether microorganisms can cooperatively combat heat-induced damages at high temperatures. Here, we use the budding yeast *Saccharomyces cerevisiae* to show that cells can help each other and their future generations to survive and replicate at high temperatures. As a consequence, even at the same temperature, a yeast population can exponentially grow, never grow or grow after unpredictable durations (hours to days) of stasis, depending on its population density. Through the same mechanism, yeasts collectively delay and can eventually stop their approach to extinction, with higher population densities stopping faster. These features arise from yeasts secreting and extracellularly accumulating glutathione—a ubiquitous heat-damage-preventing antioxidant. We show that the secretion of glutathione, which eliminates harmful extracellular chemicals, is both necessary and sufficient for yeasts to collectively survive at high temperatures. A mathematical model, which is generally applicable to any cells that cooperatively replicate by secreting molecules, recapitulates all of these features. Our study demonstrates how organisms can cooperatively define and extend the boundaries of life-permitting temperatures.

Microorganisms live in a range of habitable temperatures[1–3]. The conventional view is that increasing the temperature above an optimal value causes microorganisms to take more time to self-replicate and that—once the temperature goes beyond the habitable range, into an 'unlivable temperature' regime—microorganisms cannot replicate and they die[1–4] (Fig. 1a,b). In this textbook view, the ability of a microorganism to replicate at high temperatures is dependent on whether it can remedy heat-induced damages by itself, such as misfolded proteins[5–8]; it cannot combat these damages at sufficiently high temperatures, leading to its death (Fig. 1c). However, a microorganism often lives with other cells rather than alone, enabling them to work together for their collective survival[9–13]. Given the timeliness of understanding how the rising global temperatures affect organisms, we used the budding yeast *S. cerevisiae* to re-examine the conventional picture—one in which yeasts autonomously combat heat shocks—to investigate whether microorganisms can also collectively combat high temperatures to avoid becoming extinct (Fig. 1d).

As our starting point, we reproduced the well-known textbook picture of how temperature affects microbial growths by measuring the population-level growth rates for a laboratory-standard (wild-type) strain of haploid budding yeast in liquid cultures[4,14–16] (Fig. 1b, Supplementary Fig. 1). In this picture, the population growth rate is zero for temperatures of 40 °C and higher (Fig. 1b, Supplementary Fig. 1). Despite being evidently true—as we reproduced it here—we discovered that this textbook picture (Fig. 1c) is misleading and requires a revision. Here we revised this picture with experiments and a mathematical model, which reveal that, at sufficiently high temperatures, yeasts secrete and extracellularly accumulate glutathione—an important antioxidant for many species—that cleanses the extracellular environment of harmful reactive oxygen species, the high reactivity of which is damaging for cells. Thus, we discovered that yeasts help each other and their future generations to replicate, survive and avoid becoming extinct at high temperatures (Fig. 1d). In brief, our work demonstrates the habitability of a temperature for a single-celled organism emerging as a community-level property, determined by interactions among the members of the microbial community.

Results

Population density determines the replicability of cells and habitability of temperature. We re-examined the conventional cell-autonomous picture by incubating populations of wild-type yeasts in liquid medium at a conventionally defined habitable temperature (~38 °C), unlivable temperature (~40 °C) and a transition temperature in between the two (~39 °C). Here, in contrast with the conventional picture (Supplementary Fig. 1), we precisely set the initial population density (number of cells per ml) and studied its effect on population growth. Using a flow cytometer, we counted the integer numbers of cells per volume to determine the population density over time. These experiments revealed surprising behaviours. Specifically, at the supposedly habitable temperature of ~38 °C, none of the replicate populations that started with a relatively low population density (200 cells per ml) grew at all during incubation for ~12 d, except for a small, transient growth that occurred for a few hours immediately after the transfer from 30 °C (Fig. 2a, red curves). At the same temperature (~38 °C), setting the initial population density to be 5× larger (1,000 cells per ml) yielded a population whose behaviour was completely unpredictable—it could either grow until it reached the carrying capacity (that is, ~10^7 cells per ml) or not grow at all after the initial transient growth (Fig. 2a, green curves). In cases in which the population did grow, it could wait 4 d or 8 d or some other, unpredictable, time before starting to grow (Fig. 2a, multiple green curves). Still at the same temperature (~38 °C), setting the initial population density to be a further 5× larger (5,000 cells per ml) yielded populations that always grew exponentially and identically over time up to the carrying capacity (Fig. 2a, blue curves). Thus, at the supposedly habitable temperature of 38 °C,

[1]Kavli Institute of Nanoscience, Delft University of Technology, Delft, the Netherlands. [2]Department of Bionanoscience, Delft University of Technology, Delft, the Netherlands. [3]CIFAR, CIFAR Azrieli Global Scholars Program, Toronto, Ontario, Canada. ✉e-mail: h.youk@tudelft.nl

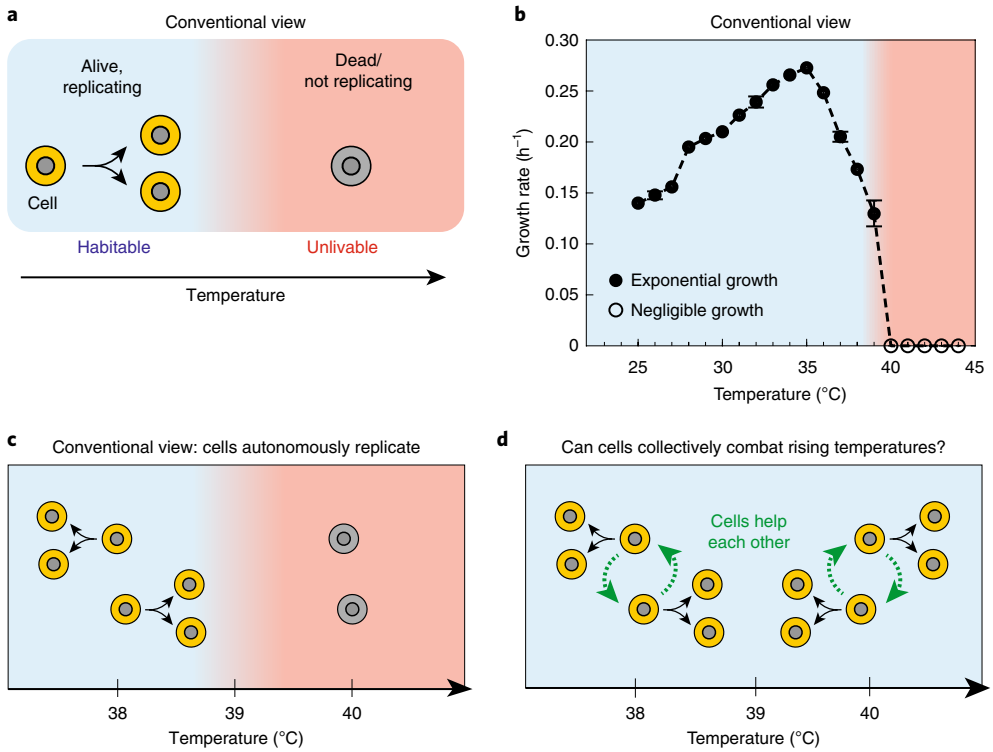

Fig. 1 | Conventional cell-autonomous view of temperature-dependent cell replication. a, The conventional view states that cells autonomously replicate at habitable temperatures (blue) and that at sufficiently high temperatures (that is, unlivable temperatures), cells fail to replicate and can eventually die (red). **b**, Growth rate as a function of temperature for populations of wild-type yeast cells. The black data points in the blue region show populations with sustained, exponential growth over time and the white data points in the red region show populations without sustained exponential growth. Data are mean ± s.e.m.; $n = 3$ replicates per data point; 39 °C is near a boundary of blue and red regions (Supplementary Fig. 1). **c**, The conventional view (explained in **a**) applied to budding yeast, on the basis of the data in **b**. **d**, The question that we investigated in our study: can microorganisms collectively combat rising temperatures so that they can turn a temperature that is unlivable (for example, 40 °C shown in **c**) into a habitable temperature?

only the largest of the three initial population densities led to the deterministic growth that the conventional picture states should be exhibited by every population[1,14–16]. The same three population-density-dependent growth behaviours also occur near to the upper limit of the habitable temperatures (~39 °C; Fig. 2b). Moreover, we found that populations with a sufficient number of cells can grow at ~40 °C—a supposedly unlivable temperature (Fig. 2c, non-red curves). These results show that, to determine whether a yeast-population grows or not, one must know both the temperature and the initial population density.

A phase diagram summarizes population-level behaviours across temperatures. By incubating liquid cultures of populations with differing initial densities at multiple temperatures, we constructed a phase diagram (Fig. 2d, Supplementary Figs. 3 and 4). The phase diagram, which summarizes the population-level growth behaviours, consists of four phases—deterministic growth, random growth, no growth and no growth due to insufficient nutrients—as a function of the initial population density and temperature. It reveals that the conventional picture (Fig. 1b,c) mistakenly arises because one typically sets the initial population density to lie within a narrow range when studying population growths. This leads to, for example, the growth rate appearing to decrease as the temperature increases within a given range (for example, ~36.5–39 °C; Fig. 1b). However, for the same temperature range, we found that the growth rates of the populations—when they grew—were poorly correlated with temperature and could vary considerably among populations, even for the same temperature in cases in which we widely varied the initial population density (Fig. 2e). The phase boundary between the deterministic-growth and random-growth phases (Fig. 2d) describes the minimum, initial population density that is necessary to guarantee that a population grew at each temperature. By contrast, the phase boundary between the random-growth and no-growth phases (Fig. 2d) describes the maximum, initial population density that is necessary to guarantee that a population never grew at each temperature. Both of these values are highly sensitive to temperature (for example, a ~100-fold change when going from 39 °C to 40 °C (Fig. 2d)). The random-growth phase may be seen as a hybrid of the deterministic-growth and no-growth phases. A small change of either temperature or initial population density can transform a no-growth into a deterministic-growth and vice versa (Fig. 2a). Interestingly, all phase boundaries converge at a single point (fold-bifurcation point) located at 40.3 °C, leading to only the no-growth phase at temperatures above 40.3 °C (Fig. 2d). Specifically, at temperatures higher than 40.3 °C, populations can grow but stop growing before reaching the carrying capacity; their final population densities depend on their initial population densities. The term fold-bifurcation point comes from dynamical systems theory and is the point in the phase diagram at which a stable fixed point (carrying capacity) merges with an unstable fixed point (the upper boundary of the no-growth phase).

Expressing a superfluous gene reshapes the phase diagram. We discovered that forcing yeasts to constitutively express the green fluorescent protein (GFP), which serves no function for cell growth, shifts the phase boundaries (Fig. 2f, Supplementary Fig. 5).

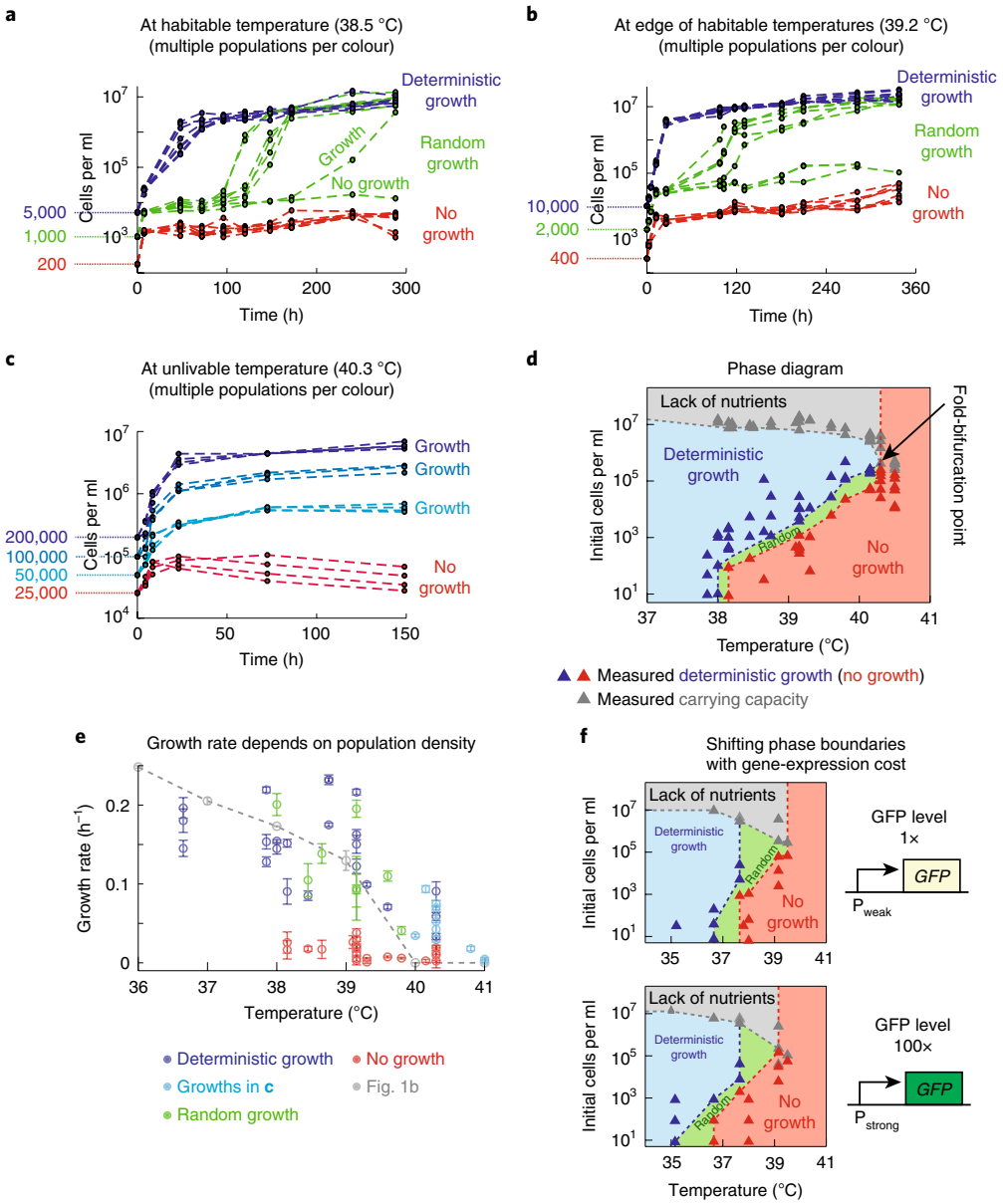

Fig. 2 | Population density determines the replicability of cells and habitability of each temperature. a–c, Population density (number of cells per ml) measured over time using a flow cytometer for populations of wild-type yeast of differing initial population densities at a conventionally defined habitable temperature (**a**; 38.5 °C); near the boundary of conventionally defined habitable and unlivable temperatures (**b**; 39.2 °C); and at a conventionally defined unlivable temperature (**c**; 40.3 °C). Figure 1b sets the conventional definition of the habitability of the temperatures. For **a** and **b**, each colour shows $n = 8$ populations that start with the same density. The red curves show no growths beyond initial transient growths (that is, no growth). The green curves show unpredictable growth (that is, random growth). Blue curves show deterministic, exponential growth whereby all of the populations grow identically (that is, deterministic growth). For **c**, Each colour shows $n = 4$ populations with the same initial population density. All of the colours except for the red show growth by around tenfold. **d**, A phase diagram constructed from measurements. The colours of regions and triangles represent the behaviours described in **b** as follows: deterministic growth (blue), random growth (green), no growth (red) and populations not growing because they have more cells than the carrying capacity (grey). Each triangle represents an experiment of the type shown in **a**–**c**; details are provided in Supplementary Figs. 3 and 4. **e**, Growth rates of populations in the no-growth phase (red), random-growth phase (green) and deterministic-growth phase (blue, light blue for growths in **c**) as a function of temperature. Data are mean ± s.e.m.; $n = 6$ or more replicates per data point for temperatures below 40 °C, and $n = 3$ for temperatures above 40 °C. Grey data and curve are from Fig. 1b. **f**, Phase diagrams constructed for engineered yeast strains that constitutively express *GFP* at the indicated levels (1×(weak promoter p*KEX2*) and 100×(strong promoter p*GPD1*)). The triangles indicate experimental data. As the genetic background of the wild-type strain is slightly different from that of GFP-expressing strains, compare the 1×GFP strain with the 100×GFP strain only (Supplementary Fig. 5).

In particular, reducing the expression of GFP could shift the phase boundaries by several degrees Celsius, suggesting that the cost of expressing superfluous genes can substantially alter the phase diagram. In light of previous studies[17,18], this may be due to GFP expression shifting the intracellular resources—which may be especially crucial for surviving at high temperatures—away from performing functions that are involved with cell growth. Although our study has revealed a genetic means for reshaping the phase diagram, the molecular mechanisms that underlie the reshaping require future studies.

A few cells initiate population growth in random-growth phase and transiently replicating subpopulations exist in non-growing populations. We turned to single-cell-level measurements for further insights. The wild-type strain has a mutated *ade2* gene that causes a cell to accumulate a red pigment, which can be diluted only by persistent cell divisions[19]. We could therefore use the red-fluorescence detector of our flow cytometer to determine which cells had been replicating and which cells had not (Extended Data Fig. 1)[20]. For a deterministically growing population, we discovered that, after a short transient growth associated with the transfer from 30 °C to the high temperature, the number of replicators exponentially increased over time up to the carrying capacity (Extended Data Fig. 1). By contrast, for random-growth and no-growth populations, the number of replicators typically decreased until very few cells (~1–5% of the population) remained as replicators. Subsequently, the number of replicators either spontaneously increased by orders of magnitude after an unpredictable number of hours or days (random-growth) or remained sustainably low and fluctuated by few-fold over nearly a week (no growth; Extended Data Fig. 1). These fluctuations were sufficiently small such that the total population density remained nearly constant. These results establish that a small subpopulation of transiently replicating cells exist and that the fraction of replicators in the population could stably remain in low numbers (for example, ~1% of total population). Below, we return to these features using a mathematical model that recapitulates them.

Cells collectively combat extinctions at high temperatures. We next investigated whether cell death, similar to cell replication, also depends on the initial population density. At several temperatures, we measured how the number of surviving cells changed over time for populations in the no-growth phase (Supplementary Fig. 6). Surprisingly, these measurements deviated qualitatively, not only quantitatively, from the textbook picture in which microorganisms such as yeasts autonomously die, dictating that the number of survivors should exponentially decrease over time[4] (Fig. 3a, brown line). We discovered that the number of survivors decreases over time in a heavy-tailed (power-law-like) manner (Fig. 3a, blue curve). In other words, the population continuously decelerates and, eventually, would cease its approach to extinction. For example, after 3 d at 41 °C, the number of survivors in a population deviated by around 10^7-fold from the expected value dictated by the conventional theory (Fig. 3a, final time point; Supplementary Fig. 6). Moreover, we discovered that the rate at which cells die at high temperatures depends on the initial population density (Fig. 3b, Supplementary Fig. 6). Specifically, the number of survivors appears to exponentially decrease during the first day before it noticeably enters a heavy-tailed decay regime on later days (Fig. 3b). We can therefore assign a constant rate of decay to each population to describe how the number of survivors initially decreases (for example, during the first day at a high temperature). We found that this rate (initial death rate) decreases as the initial population density increases, meaning that the number of survivors decreases more slowly for higher initial population densities (Fig. 3b, the three dashed lines). These results suggest that cells have a highly nonlinear, cooperative effect on each other's survival.

The temperature of the fold-bifurcation point separates two extinction-avoidance regimes. We next measured the initial death rate at multiple temperatures for populations of differing initial densities. The population half-life, which is derived from the initial death rate and is the time taken for the number of survivors to be halved, should be independent of the initial population density, according to the conventional view in which yeasts autonomously die (Fig. 3c). Instead, we discovered that increasing the initial population density always increases the population half-life and that the temperature determines how sensitively the population half-life depends on the initial population density (Fig. 3d). Specifically, a population half-life has two regimes of sensitivities. Temperatures below 40.3 °C exhibit the first regime. Here the population half-life is highly sensitive to the initial population density—it increases from hours to days if the initial population density nearly doubles (Fig. 3d, yellow curves for ~39–40 °C). Moreover, as the initial population density keeps increasing, the population half-life keeps increasing and eventually becomes infinite. This is because a sufficiently high-density population grows at these temperatures (Fig. 2d). Temperatures above 40.3 °C exhibit the second regime—increasing the initial population density above some value minimally changes the population half-life, which eventually plateaus at a finite value as the initial population density keeps increasing (Fig. 3d, brown and purple curves for ~41–43 °C). This occurs because populations cannot grow regardless of their initial densities at these temperatures (Fig. 2d). At the fold-bifurcation point (Fig. 2d), the population density can remain at a nearly constant value (that is, the population half-life is infinite because the initial death rate is zero). The fold-bifurcation point is the only place in the phase diagram (at 40.3 °C with $\sim 1 \times 10^5$ cells per ml) at which the half-life of a non-growing population is infinite. In other words, a population at the fold-bifurcation point can constantly maintain its density, apparently indefinitely, unless fluctuations cause its demise. Taken together, our results establish that a yeast's death depends on the other cells in the population. Moreover, we determined that neither heat-resistant mutants nor 'persister-like' cells, such as those observed in antibiotic persistence[21], can explain our data on cell deaths (Extended Data Fig. 2).

An extracellular factor dictates cell replication at high temperatures. We next sought to uncover the mechanisms that underlie the density-dependent replications and deaths of yeasts. First, we determined that cells isolated from a growing culture and put into a fresh medium do not grow, whereas isolating the liquid medium from an exponentially growing population and transplanting a fresh population of cells into that medium causes the transplanted population to grow, even though the phase diagram indicated that the population initially had too few cells for it to grow (Fig. 4a–c, Supplementary Figs. 7 and 8). These results suggested that an instruction that dictates population growth resides in the extracellular—and not the intracellular—environment. Moreover, we confirmed that the depletion of any of the nutrients does not instruct a population to grow (Supplementary Figs. 8 and 9), indicating that it is the secretion of some factor(s) at high temperatures that induces population growths.

Yeasts secrete glutathione to help each other replicate at high temperatures. By performing a transcriptome analysis (RNA sequencing (RNA-seq)) on wild-type yeasts at different locations in the phase diagram (Supplementary Fig. 10), we uncovered gene-expression profiles that are similar to those of yeasts undergoing environmental stresses[22,23]. We hypothesized that yeasts at high temperatures may be stressed due to reactive oxygen species, which are known to be abundant at high temperatures[24–26] and damaging for cells[27–29]. Given that antioxidants inactivate reactive oxygen species, we further hypothesized that yeasts at high temperatures may be secreting antioxidants. Indeed, studies have found that heat-shocked yeasts produce and maintain increased levels of intracellular glutathione[24,25], a tripeptide that is the yeast's primary antioxidant[24,30,31] in addition to having other essential functions[32]. Although much is known about the intracellular functions of glutathione in yeast[30–35], little is known about whether yeasts secrete glutathione and, if so, why and when they would do so aside from a few examples, such as yeasts secreting glutathione to defend against harmful extracellular arsenite[36].

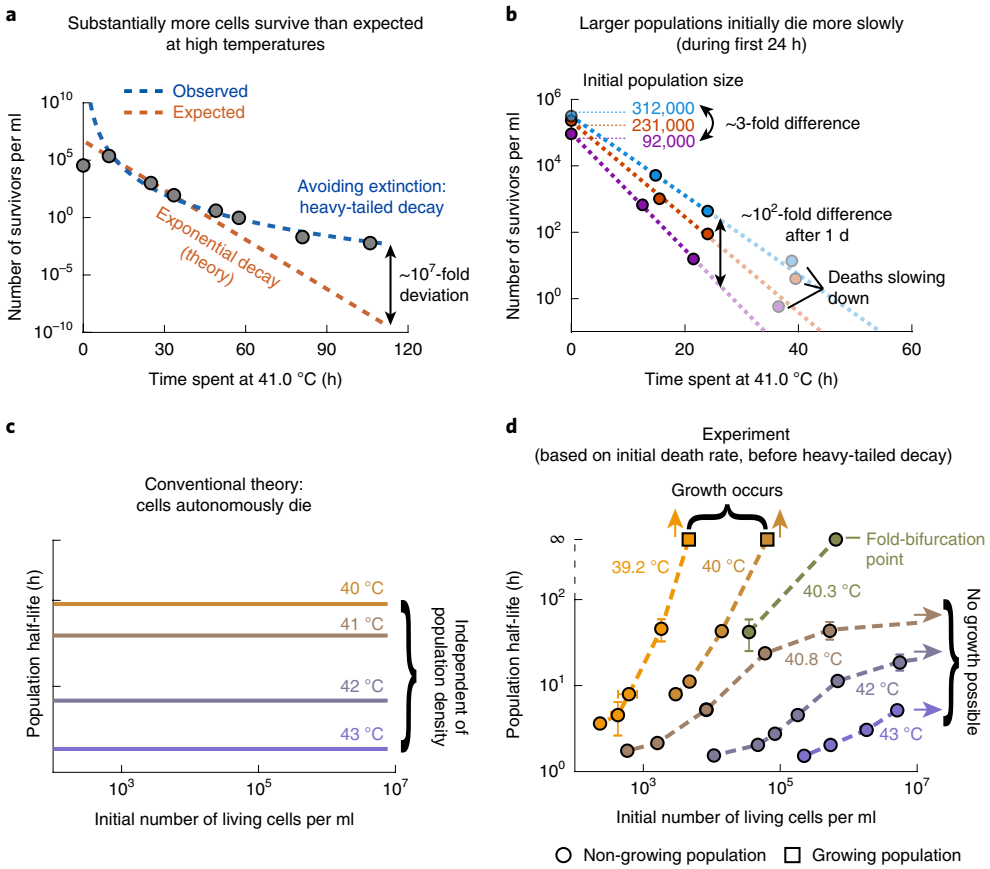

Fig. 3 | Cells collectively combat death to avoid extinction high temperatures. a, The number of survivors per ml (circles) over time in a non-growing wild-type population at 41.0 °C. The brown line is an exponentially decaying function fitted to the initial time points (between 10 h and 40 h). The blue curve is a power-law function fitted to the same data points (Supplementary Fig. 6). **b**, The number of survivors per ml for three populations of differing initial population densities at 41.0 °C measured as described in **a**. The initial population densities, after transient growths, were 92,000 cells per ml (purple), 231,000 cells per ml (orange) and 312,000 cells per ml (blue). The dashed lines represent an exponentially decreasing function fitted to the first three time points (Supplementary Fig. 6). **c**, Scheme of the conventional view, which states that cells autonomously die and that every cell has the same probability of dying per unit time. This means that the population half-life is independent of the initial population density for every temperature. The different colours represent different temperatures as indicated. **d**, Population half-life as a function of initial population density, on the basis of fitting an exponentially decreasing function to the number of survivors per ml measured during the first 24 h of incubation (after ~20 h of transient growths due to cells coming from 30 °C and adjusting to the new temperature). The half-lives of populations at 39.2 °C, 40 °C, 40.3 °C, 40.8 °C, 42 °C and 43 °C are shown in different colours as indicated. Data are mean ± s.e.m.; $n = 3$ replicates per data point. The circles represent populations in the no-growth phase. The two squares (at 39.2 °C and 40 °C) represent populations that grew due to having sufficient population densities to trigger their own growths (Fig. 2d).

Our hypothesis is supported by the fact that yeasts are known to secrete small amounts of glutathione in stationary phase at 30 °C (after diauxic shift)[37], and that we found that medium obtained from such populations induces growth at high temperatures (Supplementary Fig. 8). Indeed, we discovered that adding high concentrations of either glutathione or ascorbic acid—both antioxidants[30]—to the growth medium caused growth of populations that, without the added antioxidants, could not have grown by themselves because they had too few cells (Fig. 4d). Thus, the extracellular antioxidants glutathione and ascorbic acid are sufficient for inducing growths in yeast populations at high temperatures. Focusing on glutathione, we found that random-growth phase and deterministic-growth phase populations continuously secreted and extracellularly accumulated glutathione during log-phase growths and stationary phase at high temperatures (Fig. 4e, Supplementary Fig. 11). However, we detected only small concentrations of extracellular glutathione that barely increased over time for no-growth phase populations at high temperatures. Moreover, consistent with the population-density-dependent growths occurring only for temperatures above ~36 °C being caused by glutathione, we found that yeasts secreted glutathione only at temperatures above ~36 °C but not below it (Fig. 2d, Supplementary Fig. 11). Furthermore, we had to add sufficiently high concentrations of glutathione to induce the growth of a population that could not grow by itself (Fig. 4f). Specifically, if the extracellular glutathione concentration was less than ~0.3 µM, populations grew minimally. By contrast, extracellular glutathione concentrations of more than ~0.3 µM induced population growths up to the carrying capacity. Consistent with these findings, when we did not add any glutathione at high temperatures, no-growth populations accumulated less than ~0.3 µM of extracellular glutathione whereas the growing population accumulated more than ~0.3 µM of extracellular glutathione (Fig. 4d). In summary, we have now established that yeasts at high temperatures secrete and extracellularly accumulate glutathione that—above a threshold concentration of ~0.3 µM—induces population growths (Fig. 4g).

A mathematical model recapitulates experimental data. To explain our data, we developed a stochastic, mathematical model that contains only one free parameter (Supplementary Text). In this

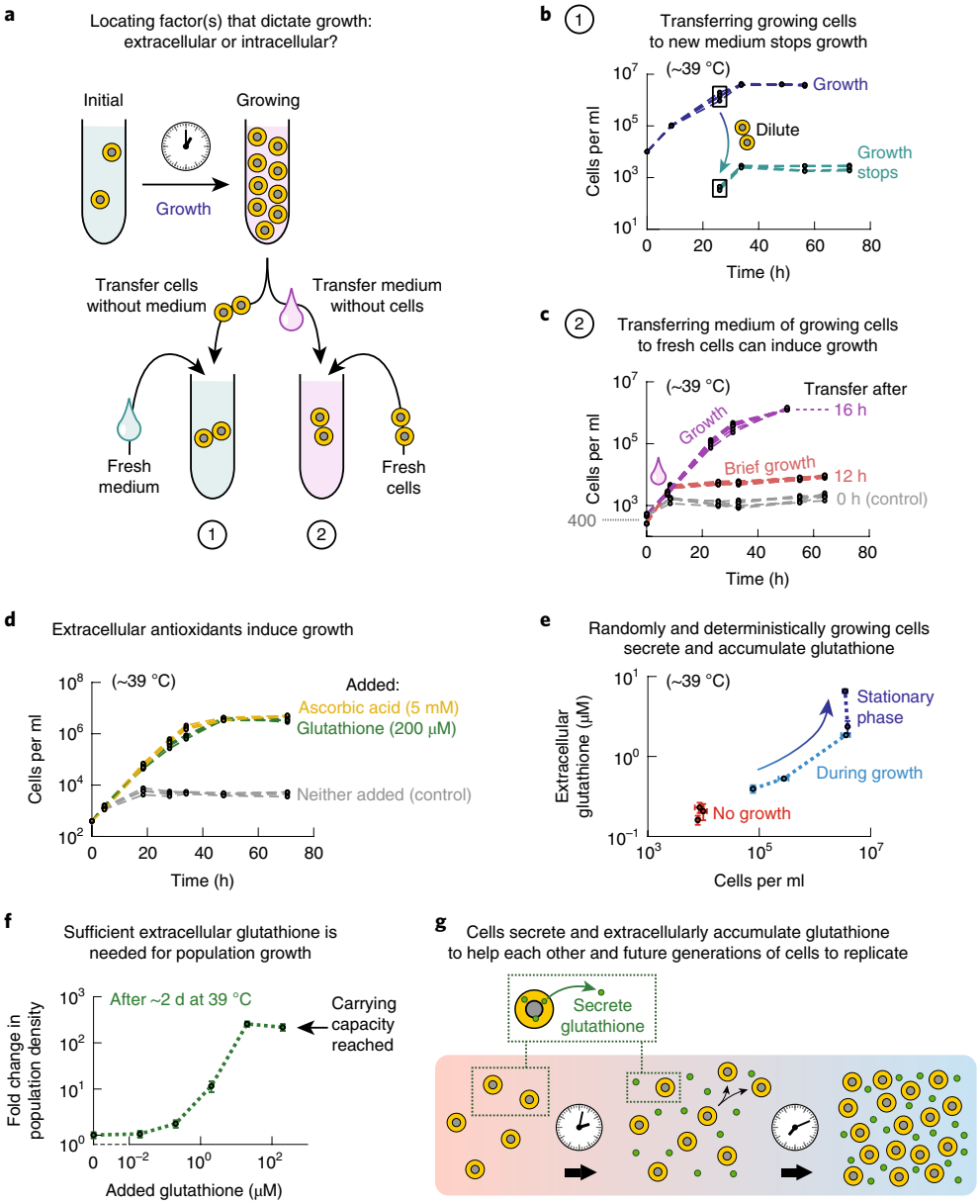

Fig. 4 | Cells secrete and extracellularly accumulate glutathione to help each other and future generations of cells to replicate at high temperatures. **a**, Schematic of the experiments for data shown in **b** and **c** to determine whether intracellular (1) or extracellular (2) factors dictate population growth. **b**, At 39.2 °C (corresponding to (1) in **a**), wild-type cells were transferred (boxed data point) from log-phase populations (blue; initial density, ~10,000 cells per ml) to fresh medium (green; initial density, ~400 cells per ml). Each colour shows $n = 4$ replicate populations (Supplementary Fig. 7). **c**, At 39.2 °C (corresponding to (2) in **a**), fresh cells from 30 °C were incubated in a growth medium that previously harboured log-phase cells at ~39 °C for 0 h (grey), 12 h (red) or 16 h (purple). Each colour shows at least $n = 6$ replicate populations (Supplementary Fig. 8). **d**, No-growth populations (initial density, ~400 cells per ml) at 39.2 °C. Adding either ascorbic acid (5 mM, yellow) or glutathione (200 μM, green) to the growth medium induces population growth. Without adding either ascorbic acid or glutathione, populations do not grow (grey). Each colour shows $n = 4$ replicate populations. **e**, The measured concentrations of extracellular glutathione (at 39.2 °C) as a function of the population density over time for no-growth (red; initial density, ~400 cells per ml), random-growth (light blue; initial density, ~2,000 cells per ml) and deterministic-growth populations (dark blue; initial density, ~10,000 cells per ml). Data are mean ± s.e.m.; $n = 3$ replicates per data point. The arrow shows both the population density and concentration of extracellular glutathione increasing together over time (Supplementary Fig. 11). **f**, Sensitivity of no-growth populations (at 39.2 °C; initial density, ~400 cells per ml) to glutathione added into the growth medium, as a function of glutathione concentration. Data are mean ± s.e.m.; $n = 4$ replicates per data point. The fold change in the population density after incubation for 2 d is shown. **g**, Scheme of the mechanism deduced in **a**–**f**. Yeast secretes and extracellularly accumulates glutathione at high temperatures, inducing population growth when its concentration reaches at least a threshold amount (~0.3 μM, from the experiment shown in **f**).

model, each living cell secretes glutathione at a constant rate and, in each time step, takes one of three actions with some probability: replicate, die or stay alive without replicating (Fig. 5a). The probability of dying is fixed by and linearly increases with temperature. Given that yeast populations require at least a threshold glutathione concentration for growth (Fig. 4f), the probability of replicating nonlinearly increases with extracellular glutathione concentration in our model (Fig. 5b). The only free parameter that required fitting

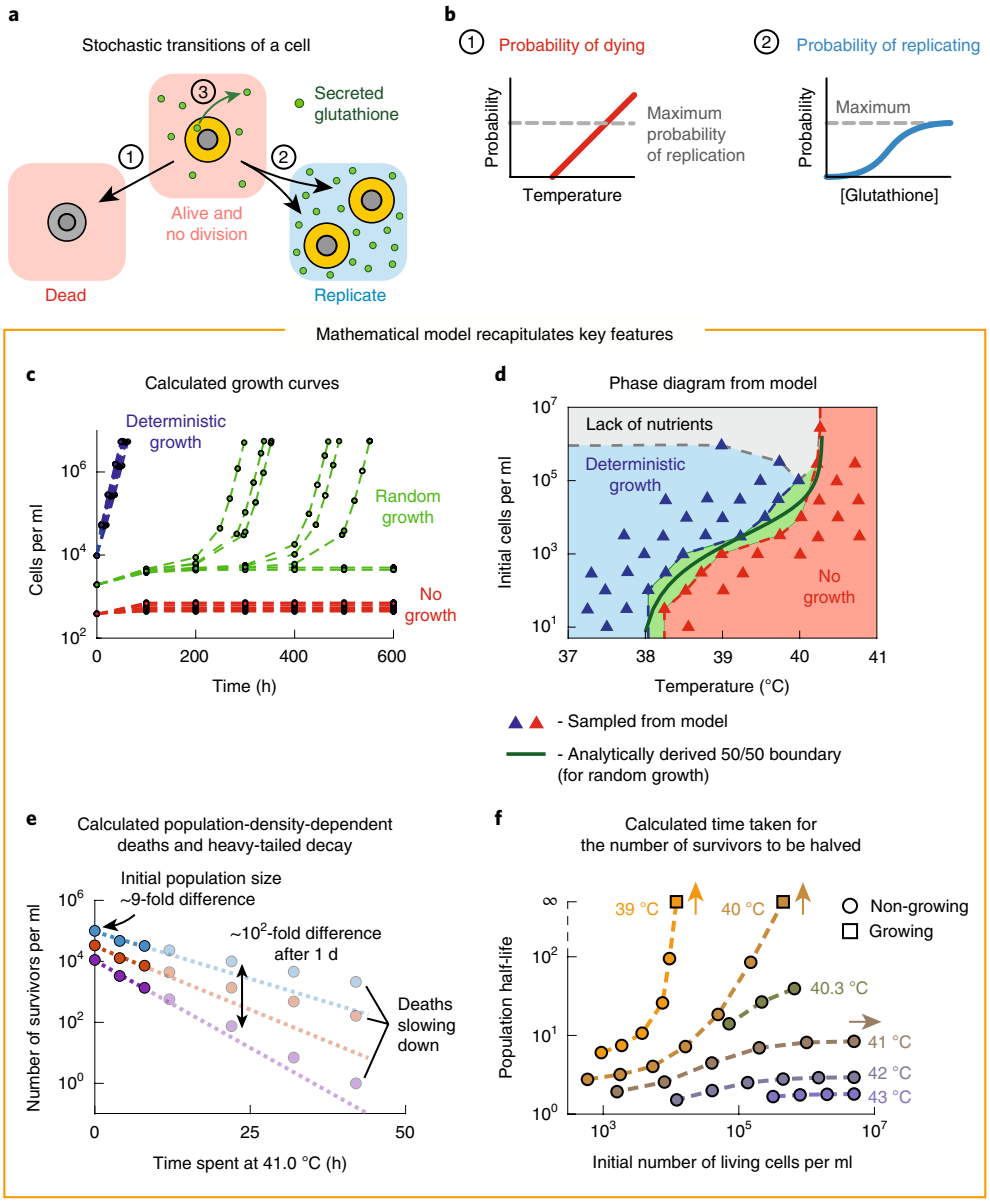

Fig. 5 | Mathematical model with one free parameter recapitulates all of the main experimental data. a,**b**, Description of the mathematical model (a full description is provided in the Supplementary Text). **a**, A cell (yellow circle) can be in three states. In each time step, any living cell either stays alive without replicating, replicates or dies. Living cells constantly secrete glutathione (green circle). **b**, Schematic of the probabilities that describe each of the transitions between the states shown in **a**. Left, the probability of a cell dying (red line) is fixed by the temperature and does not change over time. It linearly increases with temperature and, beyond some temperature, exceeds the maximum allowed value for the probability of a cell replicating (grey line). Right, the probability of a cell replicating (blue curve) nonlinearly increases with the concentration of the extracellular glutathione. **c**–**f**, Results generated by the model described in **a** and **b** with a single fixed set of parameters used for all of the panels. The model recapitulates the population-growth curves (**c**; compare with Fig. 2a); the phase diagram (**d**; compare with Fig. 2d); population-density-dependent deaths (**e**; compare with Fig. 3b); population half-life (**f**; on the basis of cell deaths during the first day of incubation; compare with Fig. 3d); the number of survivors decaying over time as a heavy-tailed function (Supplementary Fig. 12); and single-cell-level data on growths (compare Extended Data Fig. 1 with Extended Data Fig. 3). The number of replicate simulations matches that of the respective experiments (Supplementary Fig. 12).

to our data was the extracellular glutathione concentration at which the probability of replicating is half of its maximum value (Fig. 5b, blue curve). All other parameters are directly read off from our data (Supplementary Text).

Our model recapitulates all of the main experimental data (Fig. 5c–f, Extended Data Fig. 3). The main idea of the model is that, to avoid becoming extinct at a high temperature, the population—which initially lacks any extracellular glutathione and therefore starts with a zero probability of a cell replicating—must keep accumulating extracellular glutathione to keep increasing the probability of replication up to and above the probability of a cell dying, which is fixed by the temperature (Extended Data Fig. 3). Populations achieve this if and only if they start with a sufficient number of cells. Populations with too few cells go extinct and belong to the no-growth phase because they have insufficient time to accumulate enough extracellular glutathione; the probability of a cell replicating increases until the last cell dies but always remains below the probability of a cell dying. Populations with intermediate densities may grow or approach

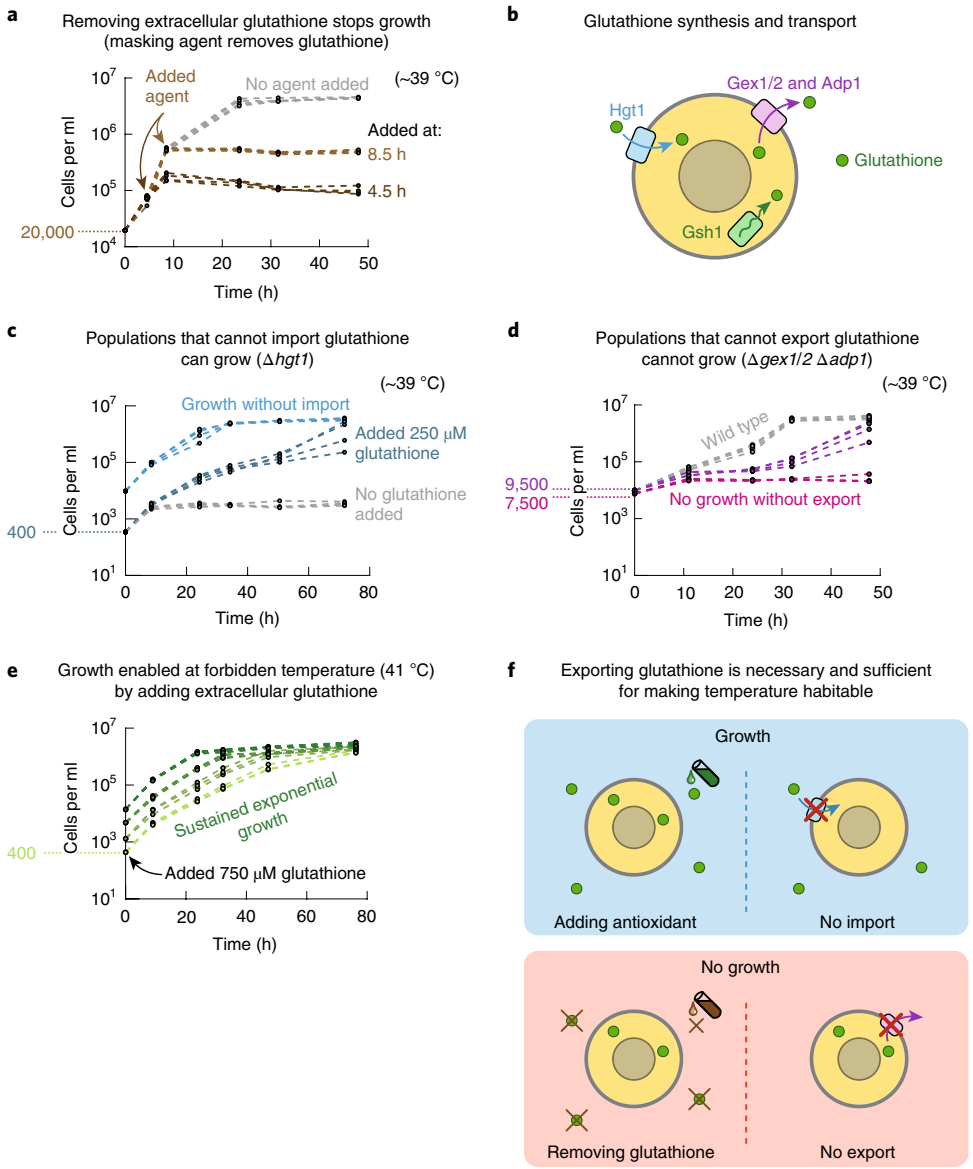

Fig. 6 | Budding yeast exports glutathione of which the extracellular, but not intracellular, role as an antioxidant enables yeast to survive high temperatures. a, Wild-type populations (at 39.2 °C; initial density for all, ~20,000 cells per ml) that should deterministically grow if left alone. A masking agent (M2VP) that inactivates extracellular glutathione was added after incubation for 4.5 h (dark brown) or 8.5 h (light brown). The grey curves show populations that did not receive the masking reagent. Each colour shows $n = 4$ replicate populations (Supplementary Fig. 13). **b**, Schematic showing how the budding yeast synthesizes, imports and exports glutathione. Glutathione is intracellularly synthesized by an enzyme that is encoded by *GSH1*. Glutathione is imported by a proton-coupled glutathione importer that is encoded by *HGT1*. Glutathione is exported by numerous exporters (not all shown), including proton antiporters encoded by *GEX1* and *GEX2* and an ATP-dependent exporter encoded by *ADP1*. **c**, The light blue curves show deterministically growing populations (at 39.2 °C) of a mutant strain (Δ*hgt1* strain) that cannot import glutathione (initial density, ~10,000 cells per ml). The grey curves show mutant populations (initial density, ~400 cells per ml) incubated without any glutathione added. Dark blue curves show mutant populations (initial density, ~400 cells per ml) incubated with 250 μM of glutathione added to the medium. Each colour shows $n = 4$ replicate populations. **d**, Populations of a mutant strain (at 39.2 °C) that lacks some of the main glutathione exporters (Δ*gex1/2* Δ*adp1* strain; initial density, ~9,500 cells per ml (purple) or ~7,500 cells per ml (pink)). Wild-type populations are shown as a comparison (grey; initial density, ~9,500 cells per ml). Each colour shows $n = 4$ replicate populations (Extended Data Fig. 4). **e**, Wild-type populations of various initial densities (at 41 °C; from ~400 cells per ml (lightest green curves) to ~14,000 cells per ml (darkest green curves)) grown in medium supplemented with 750 μM of glutathione. Each colour shows at least $n = 3$ replicate populations. **f**, The mechanisms deduced in **a**–**e**. Exporting glutathione is necessary and sufficient for yeasts to reshape the habitability of temperature. For yeast to survive and replicate at high temperatures, extracellular glutathione is (1) necessary as blocking glutathione or blocking glutathione-export stops the growth of yeast and is (2) sufficient as adding glutathione or blocking glutathione-import enables yeast to grow.

extinction (that is, exhibit the random-growth phase) because the glutathione concentration nears the threshold concentration by the time that there are very few surviving cells whose stochastic replications or deaths subsequently determine whether or not the probability of a cell replicating exceeds that of a cell dying. At temperatures above ~40.3 °C—where the fold-bifurcation is—the probability of a cell dying exceeds the maximally allowed probability of a cell replicating, meaning that only the no-growth phase is possible at these

temperatures (Fig. 5b, grey dashed line). In the no-growth phase, the continuous accumulation of extracellular glutathione results in populations decelerating their approach to extinction over time; this leads to the heavy-tailed function that describes the number of survivors decreasing over time and populations with higher initial densities more slowly approaching extinction (Supplementary Fig. 12). Taken together, our minimal model recapitulates all of the main experimental data (Fig. 5c–f).

Extracellular glutathione is necessary and sufficient to survive at high temperatures. To investigate whether extracellular glutathione is necessary—and not only sufficient (Fig. 4e,f)—for yeasts to survive at high temperatures, we used a masking reagent (1-methyl-2-vinylpyridinium (M2VP)) that specifically inactivates extracellular glutathione, without interfering with the intracellular glutathione and any other processes[38,39] (Supplementary Fig. 13). Adding the masking agent stopped deterministic growths at high temperatures (Fig. 6a). Thus, glutathione is both necessary and sufficient and is therefore the only factor that is responsible for inducing cell replications at high temperatures (above ~36.7 °C).

Manipulating the synthesis, import and export of glutathione at high temperatures. To gain further insights, we constructed mutants that were unable to synthesize glutathione (Δ*gsh1* strain; Fig. 6b)[40] or unable to import glutathione (Δ*hgt1* strain)[41] or had severely reduced ability to secrete glutathione (Δ*gex1/2* Δ*adp1* strain)[42,43]. We found that the mutants that cannot synthesize glutathione (Δ*gsh1* strain) confirmed our earlier conclusion that the wild-type cells secrete glutathione only at high temperatures (above ~36 °C; Extended Data Fig. 4). We also found that the mutants that cannot import glutathione (Δ*hgt1* strain) have the same population-density-dependent growths at high temperatures as the wild-type strain (Fig. 6c). Thus, yeasts do not need to import extracellular glutathione to replicate at high temperatures. This, in turn, means that the extracellular action of glutathione alone, and not its intracellular activity, is responsible for promoting replication at high temperatures. Indeed, we found that the mutants with significantly reduced abilities to secrete glutathione (Δ*gex1/2* Δ*adp1* strain) are less able to replicate than the wild-type strain (Fig. 6d) and, therefore, require a higher initial population density for growth. Thus, consistent with the extracellular action of glutathione—rather than the intracellular action—promoting cell replications, we found that reducing the export of glutathione reduces the ability of the populations to grow at high temperatures. Notably, we found that the mutants with reduced glutathione export (Δ*gex1/2* Δ*adp1* strain) still secreted measurable amounts of glutathione at high temperatures, which was not due to glutathione passively leaking out through cell membranes, meaning that other glutathione exporters function at high temperatures (Supplementary Fig. 14).

Yeasts can replicate at unlivable temperatures. No population can avoid extinctions at temperatures higher than 40.3 °C (Fig. 2d) because the cells die too fast to accumulate enough extracellular glutathione. Providing populations with high concentrations of glutathione at the start of incubation at extremely high temperatures may therefore help them to accumulate enough glutathione before extinction. Indeed, at 41 °C, we rescued populations with as low as 400 cells per ml from extinction; these populations grew exponentially until reaching a carrying capacity (Fig. 6e).

Discussion

By showing that secreting and extracellularly accumulating glutathione is necessary and sufficient for yeasts and their future generations to survive and replicate at high temperatures (Fig. 6f), our research revises the textbook view that cells autonomously combat heat-induced damages. A common explanation for why cells, including budding yeasts, cannot replicate at high temperatures is that essential proteins unfold at high temperatures[6]. Our research suggests that this explanation requires revisions. In fact, we found that yeasts with enough extracellular glutathione can replicate at extremely high temperatures at which such proteins would unfold (that is above 41 °C; Fig. 6e, Supplementary Fig. 12). Glutathione—an antioxidant that is essential for many organisms, including humans[30]—is central to diverse processes[31–36]. Our research extends the relatively little-known extracellular functions of glutathione in yeast[36,37] by showing that yeasts must secrete sufficient amounts of glutathione at high temperatures during log-phase growth and stationary phases. We found that glutathione extracellularly accumulates and that either ~75% (for no-growth populations) or ~25% (for growing populations) of the glutathione exists in the oxidized form (Supplementary Fig. 11). Both values, 75% and 25%, are higher than the previously reported values for oxidized glutathione that budding yeasts steadily maintain[37], suggesting that yeasts collectively clean-up their environment by reducing harmful, extracellular reactive oxygen species and thereby help each other and their future generations to replicate and survive at high temperatures.

Researchers have observed fold-bifurcation points, such as the one in our study (Fig. 2d), in other microbial populations on the verge of extinctions, such as those in which yeasts collectively hydrolyse extracellular sucrose[44–46]. These dynamic systems, including ours, typically exhibit features that are familiar from phase transitions such as 'critical slowing down'[45], which, in our study, manifests as the yeast-population's half-life being infinite at the fold-bifurcation point (Fig. 3d). By uncovering a phase diagram for cell replication, our research may aid in advancing theories of non-equilibrium statistical mechanics[47] that pertain to biologically realistic, self-replicating systems that drive and maintain themselves out of thermal equilibrium. Moreover, investigating how organisms can collectively combat high temperatures, such as in our study, may suggest ways to help organisms combat climate change and help us to understand how climate change impacts unicellular life and multicellular communities.

Methods

Growth medium and strains. The wild-type haploid yeast strain that we used was obtained from Euroscarf with the official strain name 20000A. It is isogenic to another laboratory-standard haploid yeast W303a, and has the following genotype: *MATa*; *his3-11_15*; *leu2-3_112*; *ura3-1*; *trp1Δ2*; *ade2-1*; *can1-100*. We built the two strains that constitutively express GFP by first using PCR to insert a functional *ADE2* gene into the locus of the defective *ade2* gene in the wild-type strain, by a homologous recombination, so that the red pigments that would have accumulated without the *ADE2* insertion no longer existed (that is, the strain can now synthesize adenine). We could therefore detect their GFP fluorescence without interference from the red pigment. After replacing the defective *ade2* locus with a functional *ADE2* sequence, we constructed the 1×GFP and 100×GFP strains (Supplementary Fig. 5a, GFP expression levels) by integrating a single copy of an appropriate, linearized yeast-integrating plasmid at the *his3* locus on the chromosome. Specifically, the 1×GFP strain had its GFP expression controlled by the constitutive promoter of yeast *KEX2* (621 bases upstream of its open reading frame), which was on a yeast-integration plasmid[48] that constitutively expresses *HIS3* (from *Candida glabrata*) and integrated into the non-functional *his3* locus of the wild-type strain by a homologous recombination. The GFP expression of the 100×GFP strain was controlled by the strong constitutive promoter p*GPD1* (ref. [48]), which was on the same plasmid as described for the 1×GFP strain, except that the *KEX2* promoter was swapped with the *GDP1* promoter. We cultured all yeasts in defined, minimal medium consisting of yeast nitrogen base medium, complete supplement mixture, which contained all of the essential amino acids and vitamins, and glucose at a saturating concentration (2% = 2 g per 100 ml) (all obtained from Formedium). The agar pads, which we used for growing yeast colonies, contained 2% agar (VWR Chemicals), yeast extract and peptone (YEP; Melford Biolaboratories), and 2% glucose.

Growth experiments. In a typical growth experiment, we first picked a single yeast colony from an agar plate and then incubated it at 30 °C for around 14 h in 5 ml of minimal medium, which contained all of the essential amino acids and

a saturating concentration of glucose (2%). We next took an aliquot of a defined volume from the 5 ml culture (typically 20 µl) and then flowed it through a flow cytometer (BD FACSCelesta with a High-Throughput Sampler) to determine the population density of the 5 ml culture (number of cells per ml). We then serially diluted the culture in fresh minimal medium to a desired initial population density for a growth experiment at various temperatures. Specifically, we distributed 5 ml of diluted cells into individual wells of a 'brick' with 24 10 ml wells (24 well × 10 ml assay collection & analysis microplate, Whatman). This ensured that we had eight identical replicate cultures for each initial population density (for example, Fig. 2a–c). We sealed each brick with a breathable film (Diversified Biotech, Breathe-Easy), covered it with a custom-made Styrofoam cap for insulation, and incubated it in a compressor-cooled high-precision thermostatic incubator (Memmert ICP260) that stably maintained the target temperature throughout the course of our growth experiments, with a typical s.d. of 0.017 °C over time (deviation measured over several days; Supplementary Fig. 2). Throughout the incubation, the cultures in the brick were constantly shaken at 400 r.p.m. on a plate shaker (Eppendorf MixMate), which we kept in the incubator. To measure the population densities, we took a small aliquot (typically 50 µl) from each well, diluted it with PBS (Fisher Bioreagents) into a 96-well plate (Sarstedt, 9020411) and then flowed it through the flow cytometer, which gave us the number of cells per ml. We determined the growth rates by measuring the maximum slope of the log-transformed population density after their initial, transient growths.

Flow cytometry. We used a BD FACSCelesta system with a High-Throughput Sampler and lasers with the following wavelengths: 405 nm (violet), 488 nm (blue) and 561 nm (yellow/green). We calibrated the FSC and SSC gates to detect only yeast cells (FSC-PMT = 681 V, SSC-PMT = 264 V, GFP-PMT = 485 V, mCherry-PMT = 498 V; as a control, flowing PBS yielded no detected events). The number of cells per ml that we plotted in our growth experiments is proportional to the number of events (yeast cells) that the flow cytometer measured in an aliquot of cells with a defined volume. We measured the GFP fluorescence using the FIT-C channel and the red cells (Extended Data Fig. 1) with the mCherry channel. We analysed the flow-cytometry data using a custom MATLAB script (MathWorks).

Measuring the number of surviving cells. For the experiments shown in Fig. 3a,b, Extended Data Fig. 2 and Supplementary Fig. 6, we prepared cultures (250 ml) of wild-type cells in 500 ml Erlenmeyer flasks. We placed a constantly spinning magnetic stir bar at the bottom of the flasks and placed each flask on top of spinning magnets (Labnet Accuplate; at 220 r.p.m.) inside the thermostatic incubators (Memmert ICP260) that we set at desired high temperatures. For the experiments shown in Fig. 3d, we prepared a brick with cultures as described in the 'Growth Experiments' section to have multiple replicate populations and to compare the different population densities. For every time point, we ensured that these populations were not growing (that is, all of the populations were in the no-growth phase after a transient growth) by using the flow cytometer to measure their population densities over time to verify that their population densities indeed remained constant over time. For the first 48 h of incubation, we measured the number of colony-forming units by taking out a small-volume aliquot from the liquid cultures at high temperatures and distributing droplets from a serial dilution of the aliquot across an agar pad (2% glucose with YEP) that we then incubated at 30 °C for several days until (no) colonies appeared. When there were few surviving cells per ml—especially for the final time points in each experiment—we determined, in parallel to the plating method, the number of colony-forming units by transferring an appropriate volume of the liquid cultures from the incubator to an Erlenmeyer flask and then diluting it with the same volume of fresh minimal medium. We sealed the flask with a breathable film (Diversified Biotech, Breathe-Easy) and then left it still without stirring on a benchtop at ~24–30 °C—we checked that slightly lower temperatures (for example, room temperatures) did not affect colony-forming abilities—which enabled any surviving cells to settle at the bottom of the flask and form colonies. We counted the number of colonies at the bottom of the flask—we plotted these values as the final time points in each experiment (Fig. 3a, Extended Data Fig. 2, Supplementary Fig. 6).

Cell-transfer experiments. We incubated a 24-well brick containing liquid cultures, each of which were in a deterministic-growth phase, at a desired temperature (for example, 10,000 cells per ml at 39.2 °C). We incubated the brick containing these liquid cultures in thermostatic incubators (Memmert ICP260) as described in the 'Growth experiments' section. About 48 h after incubation, we took aliquots from the cultures that were growing in mid-log phase (as checked using flow cytometry) and then diluted each of them into 5 ml of fresh minimal medium in 24-well bricks so that these newly created populations were in the no-growth phase at the same temperature as the original population that they came from (400 cells per ml at 39.2 °C). We sealed the 24-well brick with a breathable film (Diversified Biotech, Breathe-Easy) and then incubated them at the same temperature as the original population. We performed the growth experiments with these new populations as described in the 'Growth experiments' section.

Medium-transfer experiments. Details are also provided in Supplementary Fig. 8. At a given temperature, we first grew populations in the deterministic-growth phase (for example, initial population density of 30,000 cells per ml at 39.2 °C). We used a flow cytometer to measure their growing population densities at different times so that we knew in which part of deterministic growth they were in (for example, mid-log phase). We then transferred each liquid culture into a 50 ml tube (Sarstedt) and centrifuged it so that the cells formed a pellet at the bottom of the tube. We then took the resulting supernatant, without the cell pellet, and flowed it through filter paper with 200-nm-diameter pores (VWR, 150 ml Filter Upper Cup) to remove any residual cells from the supernatant. After filtering, we flowed an aliquot of the filtered medium through a flow cytometer to verify that there were no cells left in the filtered medium. We incubated fresh cells into the filtered medium (rather than into fresh minimal medium) and proceeded with a growth experiment at the desired temperature as described in the 'Growth experiments' section.

Measuring the depletion of extracellular nutrients. Details are also provided in Supplementary Fig. 9. We prepared various growth media by diluting the minimal medium (SC media) by various amounts with water. These diluted SC media were each supplemented with 2% glucose. We next incubated fresh cells in these diluted SC media at the desired temperature (such as 39.2 °C) as described in the 'Growth experiments' section. We compared populations of cells that initially had 400 cells per ml (this corresponds to a no-growth phase; Fig. 2d) with populations that initially had 10,000 cells per ml (this corresponds to a deterministic-growth phase; Fig. 2d) to confirm that cells were still able to grow in these media. Similarly, we also varied the amounts of glucose that we supplemented the SC medium with.

RNA-seq. For each temperature that we studied, we collected cells in 50 ml tubes and centrifuged them using a precooled centrifuge. We then extracted RNA from each cell pellet using the RiboPure Yeast Kit (Ambion, Life Technologies) according to its protocol. We next prepared the cDNA library with the 3′ mRNA-Seq library preparation kit (Quant-Seq, Lexogen) according to its protocol. We then loaded the cDNA library onto an Illumina MiSeq system using the MiSeq Reagent Kit c2 (Illumina) according to its protocol. We analysed the resulting RNA-seq data as previously described[49]. We performed the read alignment using TopHat, read assembly using Cufflinks and analyses of differential gene expression data using Cuffdiff. We used the reference genome for *S. cerevisiae* from ensembl. We categorized the genes by the Gene Ontologies with AmiGO2 and manually checked them with the Saccharomyces Genome Database.

Measuring the concentration of extracellular glutathione. To quantify the concentration of extracellular glutathione, cells were removed from their liquid medium by flowing the liquid cultures that contained cells through a pore filter (0.45 µm; VWR, cellulose-acetate membrane). To ensure and verify that there were no cells remaining in the filtered medium, we flowed the filtered medium through a flow cytometer. The flow cytometer indeed did not detect any cells in the filtered medium. We measured concentrations of glutathione in the filtered medium according to the manufacturer's protocol (38185 quantification kit for oxidized and reduced glutathione, 200 tests). We used a BMG Labtech Spectrostar Nano system to measure the optical absorbance at 415 nm. As a background subtraction (blank) for all absorbance measurements, we subtracted the absorbance that we obtained by applying the assay to fresh minimal medium without any glutathione (the background absorbance could come from, for example, cysteine in the minimal medium). We subsequently determined the concentrations of extracellular glutathione by using a calibration curve that we constructed by measuring the absorbance at 415 nm for known amounts of glutathione that we added by hand into a buffer provided by the manufacturer.

Glutathione-masking experiment. We incubated a brick of liquid cultures that were in the deterministic-growth phase (20,000 cells per ml) at 39.2 °C. After some time (for example, 8.5 h afterwards), we added 750 µM of M2VP (Sigma-Aldrich, 69701), which is a thiol-scavenging agent that rapidly masks reduced glutathione[39], and proceeded with the experiment as described in the 'Growth experiments' section. Identical replicate cultures, which did not receive the M2VP, were used as a reference.

Mutant yeast strains. We constructed mutant strains that could not synthesize glutathione or could not import or export glutathione. Primers were designed using a 50–60 bp sequence that was either homologous to the 50–60 bp upstream of the start codon of the desired gene or downstream of the stop codon of the desired gene. These primers were used to amplify a selection marker by PCR, resulting in a PCR product that contained a selection marker of which the ends were homologous to the flanking regions of the gene to be knocked out. The wild-type strain (W303) was grown overnight in YPD (5 ml) in a rotator (40 r.p.m.) at 30 °C, and was subsequently transformed with the PCR fragment using standard methods of yeast cloning. The biosynthesis mutant (Δ*gsh1* strain) was constructed by removing *GSH1* from W303. The import mutant (Δ*hgt1* strain) was constructed by removing *HGT1*. The export mutant (Δ*gex1*/*2*Δ*adp1* strain) was constructed by removing, sequentially, *GEX1*, then *GEX2* and then *ADP1*. The resulting

transformants were grown on YPD selection plates, and knockouts were verified using PCR.

Measuring integrity of cell membrane. Cells of the Δ*gex1/2* Δ*adp1* strain were incubated in liquid medium at 39.2 °C (3,000–10,000 cells per ml; corresponding to a random-growth phase). We took aliquots of these cultures and then stained them with 1 μg ml^{-1} of propidium iodide (Thermo Fisher Scientific, P3566). We then flowed these stained aliquots through a flow cytometer. The flow cytometer measured the number of cells that were unstained by the propidium iodide (that is, cells whose membranes were intact[50]).

Mathematical model. Derivations of equations, a detailed description of the mathematical model and the parameter values used for simulations are provided in the Supplementary Text.

Reporting Summary. Further information on research design is available in the Nature Research Reporting Summary linked to this article.

Data availability

All data supporting the findings of this study are available within the paper and its Supplementary Information. RNA-seq data are available at NCBI GEO (GSE137151). Source data for Figs. 2–4 and 6 are provided with the paper. The data that support the findings of this study are available from the corresponding author on reasonable request.

Code availability

All scripts used for simulations in this research are publicly available (GitHub diederiklt/YeastHighTemperatures).

Received: 17 August 2019; Accepted: 6 March 2020;
Published online: 20 April 2020

References

1. Madigan, M. T., Martinko, J. M., Stahl, D. A. & Clark, D. *Brock Biology of Microorganisms* 13th edn, 162–163 (Pearson, 2011).
2. Milo, R. & Phillips, R. *Cell Biology by the Numbers* 1st edn (Garland Science, 2015).
3. Bruslind, L. *Microbiology* (Open Oregon State University, 2019).
4. Doran, P. M. *Bioprocess Engineering Principles* 2nd edn 653–655 (Academic, 2012).
5. Ghosh, K. & Dill, K. Cellular proteomes have broad distributions of protein stability. *Biophys. J.* **99**, 3996–4002 (2010).
6. Leuenberger, P. et al. Cell-wide analysis of protein thermal unfolding reveals determinants of thermostability. *Science* **355**, eaai7825 (2017).
7. Verghese, J., Abrams, J., Wang, Y. & Morano, K. A. Biology of the heat shock response and protein chaperones: budding yeast (*Saccharomyces cerevisiae*) as a model system. *Microbiol. Mol. Biol. Rev.* **76**, 115–158 (2012).
8. Richter, K., Haslbeck, M. & Buchner, J. The heat shock response: life on the verge of death. *Mol. Cell* **40**, 253–266 (2010).
9. Miller, M. B. & Bassler, B. L. Quorum sensing in bacteria. *Annu. Rev. Microbiol* **55**, 165–199 (2001).
10. Gore, J., Youk, H. & van Oudenaarden, A. Snowdrift game dynamics and facultative cheating in yeast. *Nature* **459**, 253–256 (2009).
11. Koschwanez, J. H., Foster, K. R. & Murray, A. W. Sucrose utilization in budding yeast as a model for the origin of undifferentiated multicellularity. *PLoS Biol.* **9**, e1001122 (2011).
12. Koschwanez, J. H., Foster, K. R. & Murray, A. W. Improved used of a public good selects for the evolution of undifferentiated multicellularity. *eLife* **2**, e00367 (2013).
13. Ratzke, C., Denk, J. & Gore, J. Ecological suicide in microbes. *Nat. Ecol. Evol.* **2**, 867–872 (2018).
14. Postmus, J. et al. Quantitative analysis of the high temperature-induced glycolytic flux increase in *Saccharomyces cerevisiae* reveals dominant metabolic regulation. *J. Biol. Chem.* **283**, 23524–23532 (2008).
15. Walsh, R. M. & Martin, P. A. Growth of *Saccharomyces cerevisiae* and saccharomyces uvarum in a temperature gradient incubator. *J. Inst. Brew.* **83**, 169–172 (1977).
16. Ratkowsky, D. A., Lowry, R. K., McMeekin, T. A., Stokes, A. N. & Chandler, R. E. Model for bacterial culture growth rate throughout the entire biokinetic temperature range. *J. Bacteriol.* **154**, 1222–1226 (1983).
17. Dekel, E. & Alon, U. Optimality and evolutionary tuning of the expression level of a protein. *Nature* **436**, 588–592 (2005).
18. Scott, M. & Hwa, T. Bacterial growth laws and their applications. *Curr. Opin. Biotechnol.* **22**, 559–565 (2011).
19. Bharathi, V. et al. Use of *ade1* and *ade2* mutations for development of a versatile red/white colour assay of amyloid-induced oxidative stress in *Saccharomyces cerevisiae*. *Yeast* **33**, 607–620 (2016).
20. Charlebois, D. A., Hauser, K., Marshall, S. & Balázsi, G. Multiscale effects of heating and cooling on genes and gene networks. *Proc. Natl Acad. Sci. USA* **115**, E10797–E10806 (2018).
21. Balaban, N. Q. Persistence: mechanisms for triggering and enhancing phenotypic variability. *Curr. Opin. Genet. Dev.* **21**, 768–775 (2011).
22. Causton, H. C. et al. Remodeling of yeast genome expression in response to environmental changes. *Mol. Biol. Cell* **12**, 323–337 (2001).
23. Gasch, A. P. et al. Genomic expression programs in the response of yeast cells to environmental changes. *Mol. Biol. Cell* **11**, 4241–4257 (2000).
24. Sugiyama, K., Kawamura, A., Izawa, S. & Inoue, Y. Role of glutathione in heat-shock-induced cell death of *Saccharomyces cerevisiae*. *Biochem. J.* **352**, 71–78 (2000).
25. Sugiyama, K., Izawa, S. & Inoue, Y. The Yap1p-dependent induction of glutathione synthesis in heat shock response of *Saccharomyces cerevisiae*. *J. Biol. Chem.* **275**, 15535–15540 (2000).
26. Davidson, J. F., Whyte, B., Bissinger, P. H. & Schiestl, R. H. Oxidative stress is involved in heat-induced cell death in *Saccharomyces cerevisiae*. *Proc. Natl Acad. Sci. USA* **93**, 5116–5121 (1996).
27. Yakes, F. M. & van Houten, B. Mitochondrial DNA damage is more extensive and persists longer than nuclear DNA damage in human cells following oxidative stress. *Proc. Natl Acad. Sci. USA* **94**, 514–519 (1997).
28. Cabiscol, E., Piulats, E., Echave, P., Herrero, E. & Ros, J. Oxidative stress promotes specific protein damage in *Saccharomyces cerevisiae*. *J. Biol. Chem.* **275**, 27393–27398 (2000).
29. Bilinski, T., Litwinska, J., Blaszczynski, M. & Bajus, A. SOD deficiency and the toxicity of the products of autoxidation of polyunsaturated fatty acids in yeast. *Biochim. Biophys. Acta* **1001**, 102–106 (1989).
30. Jamieson, D. J. Oxidative stress responses of the yeast *Saccharomyces cerevisiae*. *Yeast* **14**, 1511–1527 (1998).
31. Zechmann, B. et al. Subcellular distribution of glutathione and its dynamic changes under oxidative stress in the yeast *Saccharomyces cerevisiae*. *FEMS Yeast Res.* **11**, 631–642 (2011).
32. Kumar, C. et al. Glutathione revisited: a vital function in iron metabolism and ancillary role in thiol-redox control. *EMBO J.* **30**, 2044–2056 (2011).
33. Toledano, M. B., Kumar, C., Le Moan, N., Spector, D. & Tacnet, F. The system biology of thiol redox system in *Escherichia coli* and yeast: differential functions in oxidative stress, iron metabolism and DNA synthesis. *FEBS Lett.* **581**, 3598–3607 (2007).
34. Elskens, M. T., Jaspers, C. J. & Penninckx, M. J. Glutathione as an endogenous sulfur source in the yeast *Saccharomyces cerevisiae*. *J. Gen. Microbiol.* **137**, 637–644 (1991).
35. Mehdi, K. & Penninckx, M. J. An important role for glutathione and γ-glutamyltranspeptidase in the supply of growth requirements during nitrogen starvation of the yeast *Saccharomyces cerevisiae*. *Microbiology* **143**, 1885–1889 (1997).
36. Thorsen, M. et al. Glutathione serves an extracellular defence function to decrease arsenite accumulation and toxicity in yeast. *Mol. Microbiol.* **84**, 1177–1188 (2012).
37. Perrone, G. G., Grant, C. M. & Dawes, I. W. Genetic and environmental factors influencing glutathione homeostasis in *Saccharomyces cerevisiae*. *Mol. Biol. Cell* **16**, 218–230 (2005).
38. Giustarini, D. et al. Pitfalls in the analysis of the physiological antioxidant glutathione (GSH) and its disulphide (GSSG) in biological samples: an elephant in the room. *J. Chromatogr. B Analyt. Technol. Biomed. Life Sci.* **1019**, 21–28 (2016).
39. Araujo, A. R., Saraiva, M. L. & Lima, J. L. Determination of total and oxidized glutathione in human whole blood with a sequential injection analysis system. *Talanta* **74**, 1511–1519 (2008).
40. Grant, C. M., MacIver, F. H. & Dawes, I. W. Glutathione is an essential metabolite required for resistance to oxidative stress in the yeast *Saccharomyces cerevisiae*. *Curr. Genet.* **29**, 511–515 (1996).
41. Bourbouloux, A., Shahi, P., Chakladar, A., Delrot, S. & Bachhawat, A. K. Hgt1p, a high affinity glutathione transporter from the yeast *Saccharomyces cerevisiae*. *J. Biol. Chem.* **275**, 13259–13265 (2000).
42. Dhaoui, M. et al. Gex1 is a yeast glutathione exchanger that interferes with pH and redox homeostasis. *Mol. Biol. Cell* **22**, 2054–2067 (2011).
43. Kiriyama, K., Hara, K. Y. & Kondo, A. Extracellular glutathione fermentation using engineered *Saccharomyces cerevisiae* expressing a novel glutathione exporter. *Appl. Microbiol. Biotechnol.* **96**, 1021–1027 (2012).
44. Dai, L., Vorselen, D., Korolev, K. & Gore, J. Generic indicators for loss of resilience before a tipping point leading to population collapse. *Science* **336**, 1175–1177 (2012).
45. Strogatz, S. H. *Nonlinear Dynamics and Chaos: With Applications to Physics, Biology, Chemistry, and Engineering* (Westview, 1994).
46. Mojtahedi, M. et al. Cell fate decision as high-dimensional critical state transition. *PLoS Biol.* **14**, e2000640 (2016).
47. Garcia-Ojalvo, J., Sancho, J. M. & Ramirez-Piscina, L. A nonequilibrium phase transition with colored noise. *Phys. Lett. A* **168**, 35–39 (1992).

48. Youk, H. & Lim, W. A. Secreting and sensing the same molecule allows cells to achieve versatile social behaviors. *Science* **343**, 1242782 (2014).
49. Trapnell, C. et al. Differential gene and transcript expression analysis of RNA-seq experiments with TopHat and Cufflinks. *Nat. Protoc.* **7**, 562–578 (2012).
50. Riccardi, C. & Nicoletti, I. Analysis of apoptosis by propidium iodide staining and flow cytometry. *Nat. Protoc.* **1**, 1458–1461 (2006).

Acknowledgements

We thank S. Itzkovitz and A. Raj for comments on our manuscript; the members of the Youk laboratory for helpful discussions; and M. Mohebbi for help with initial experiments. H.Y. was supported by the European Research Council (ERC) Starting Grant (MultiCellSysBio, no. 677972), the Netherlands Organisation for Scientific Research (NWO) Vidi award (no. 680-47-544), the CIFAR Azrieli Global Scholars Program and the EMBO Young Investigator Award.

Author contributions

H.Y. initiated this research and performed the initial growth experiments. D.S.L.T. subsequently designed additional experiments with guidance from H.Y. D.S.L.T. performed all of the experiments, developed the mathematical model and analysed the data with advice from H.Y. D.S.L.T. and H.Y. discussed and checked all of the data and wrote the manuscript.

Competing interests

The authors declare no competing interests.

Additional information

Extended data is available for this paper at https://doi.org/10.1038/s41564-020-0704-2.

Supplementary information is available for this paper at https://doi.org/10.1038/s41564-020-0704-2.

Correspondence and requests for materials should be addressed to H.Y.

Reprints and permissions information is available at www.nature.com/reprints.

Publisher's note Springer Nature remains neutral with regard to jurisdictional claims in published maps and institutional affiliations.

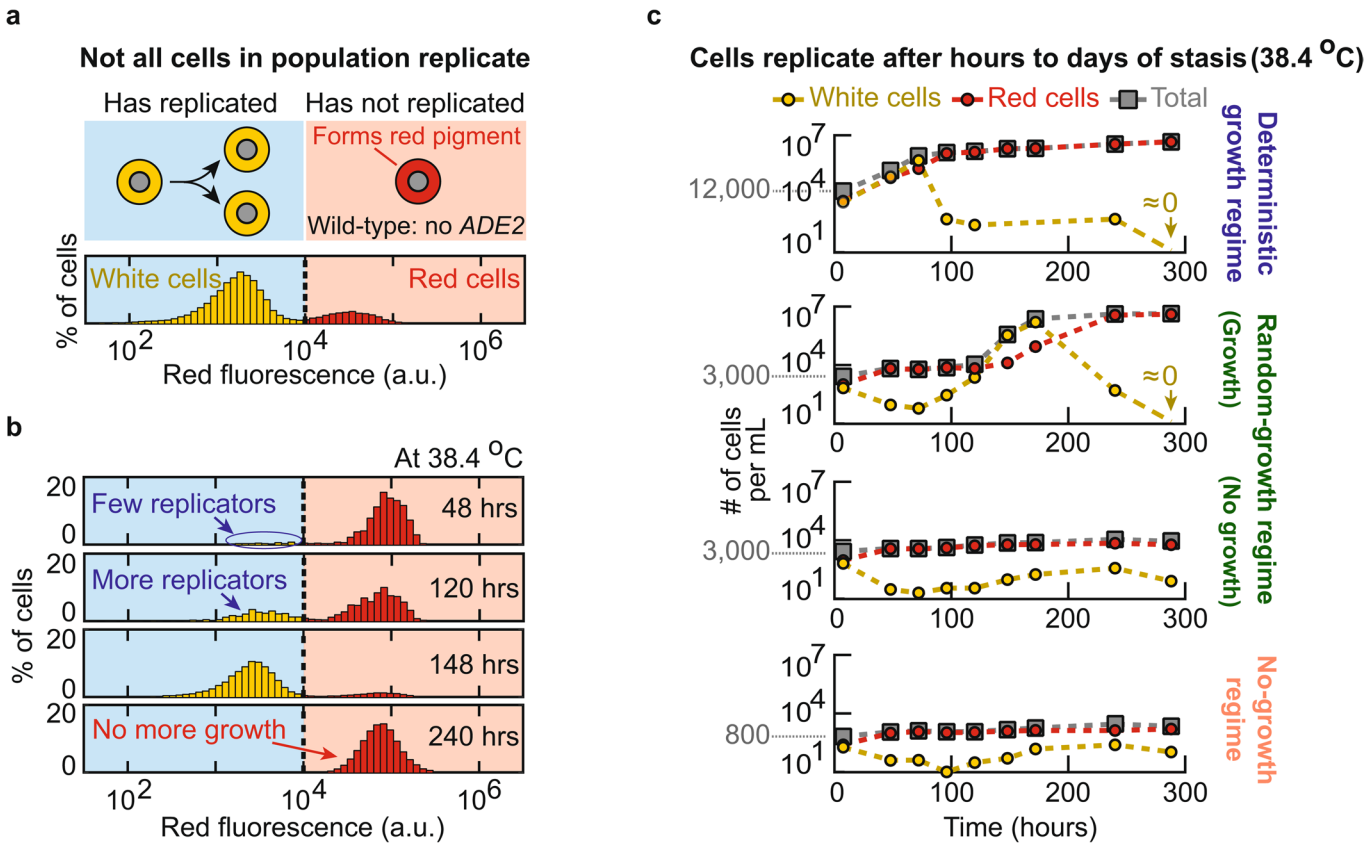

Extended Data Fig. 1 | A few cells stochastically and transiently replicate within populations that are in either no-growth or random-growth phase (Related to Fig. 2a–d). a, The wild-type strain lacks a functional *ADE2* gene for synthesizing adenine. Since we incubated yeasts in the minimal media with all the essential nutrients - including adenine - the wild-type cells were still capable of growing. But having a defective *ade2* gene turns yeasts red if they have not divided for some time because they have accumulated red pigments - these are by-products of the not-fully-repressed and defective adenine-biosynthesis. The cells can only dilute away the red pigments through cell divisions. The histogram shows percentages of red cells (non-replicators) and 'white cells' (non-red, replicators) in a population, determined by a flow cytometer's red-fluorescence detector that quantified redness of individual cells. **b**, Percentage of white and red cells over time measured with the flow cytometer for a population of wild-type yeasts. Time shows hours of incubation in 38.4 °C. These histograms show example time courses for a population that grew at a high temperature. **c**, Numbers of white and red cells in a population per ml, at various times for three different growth regimes indicated by the phase diagram (Fig. 2d). Random-growth phase shows two replicate populations - one growing (second row) and one not growing (third row).

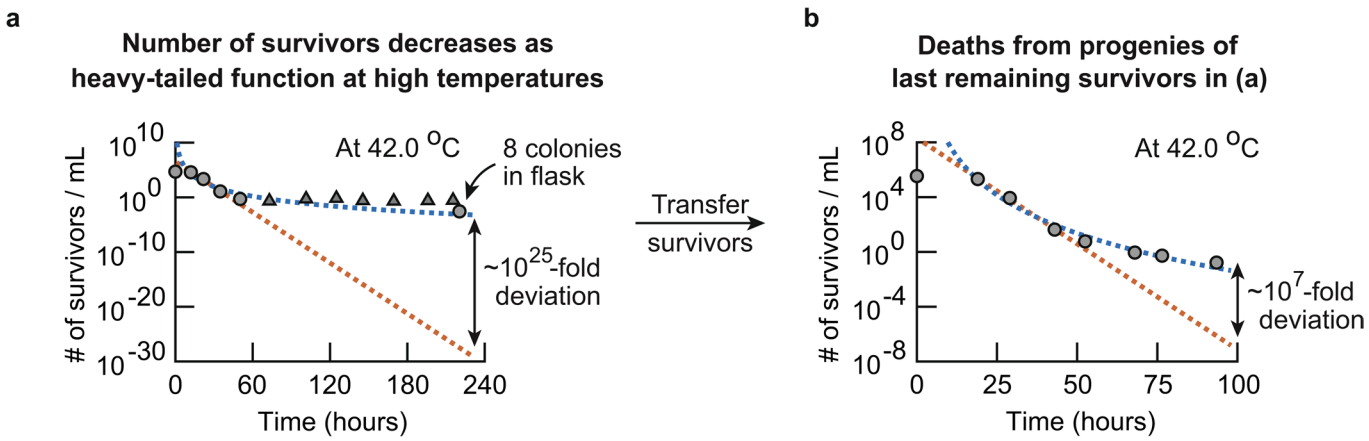

Extended Data Fig. 2 | The number of survivors decreasing over time as a heavy-tailed function is not due to heat-tolerant mutants or persistor-like cells existing within a population (Related to Fig. 3a, b). a-b, The number of survivors per ml over time for populations of wild-type cells kept in the no-growth phase at 42.0 °C (Supplementary Fig. 6). The brown dashed lines represent an exponentially decaying function fitted to the data points that lie between 10 h and 50 h. The blue dashed curve is a power-law function fitted to the same data points. **a**, The number of surviving wild-type cells. Triangles are overestimates (i.e., the aliquots taken from the liquid culture at 42 °C did not yield any colonies on agar at 30 °C, so there could not have been more survivors in the liquid culture than values represented by the triangles). We observed eight colonies formed at the last time point (~220 h - the last circle). **b**, We took one of these eight colonies - progenies of the survivors from the last time point in **a** - and used the cells from this colony to repeat the experiment. The number of survivors in this new experiment also decreased over time as a heavy-tailed function. This result eliminates the possibility that the survivors of the high temperature (42 °C) in the first experiment **a** are either heat-tolerant mutants or persistor-like cells that behave similarly to persistors of antibiotic treatments. To see this, suppose that the survivors at the last time point in **a** were heat-tolerant mutants or persistor-like cells. Then the starting population in **b** must be a pure population of these heat-tolerant mutants or persistor-like cells, that would have died at a slower rate than all the other cells of the wild-type population that started in **a**. It then follows that the number of survivors per ml in **b** should decrease as a single, slowly decaying exponential function rather than decreasing over time as a heavy-tailed function. Thus, by contradiction, the survivors at high temperatures are not heat-tolerant mutants or persistor-like cells.

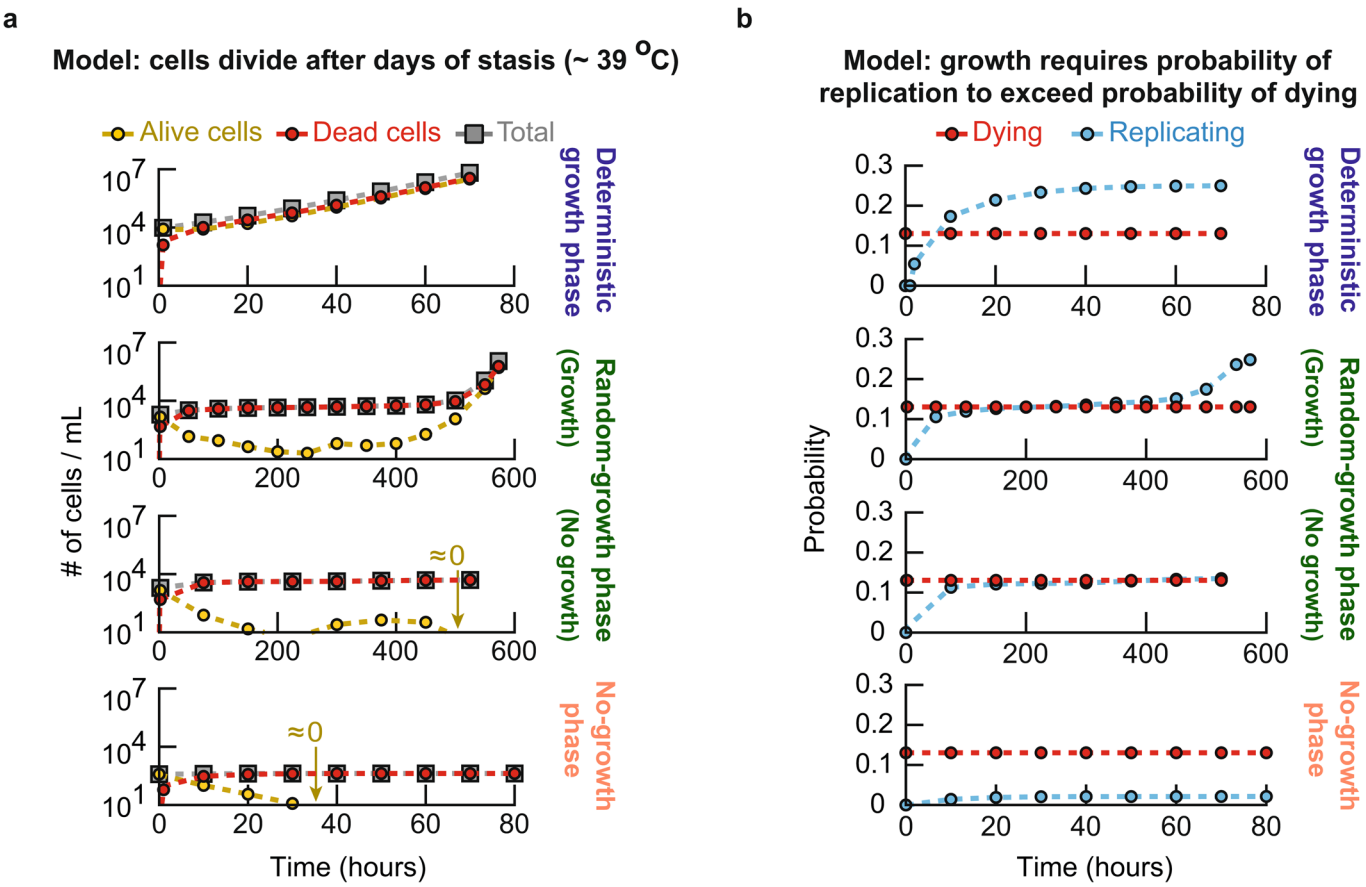

Extended Data Fig. 3 | Mathematical model reproduces the sustained population of few replicating cells in random-growth and no-growth phases (Related to Extended Data Fig. 1). a, The number of alive (yellow) and dead cells (red) over time. The same, fixed set of parameters was used as in Fig. 5. Depending on the initial population density, the number of alive cells grows exponentially (top row - deterministic-growth phase) or decreases exponentially until extinction (bottom row - no-growth phase). For intermediate population densities (2nd and 3rd rows - random-growth), the population is very sensitive to the stochastic transitions of very few alive cells (at ~300 h). Based on whether these cells stay alive without replicating, replicate, or die in the next time steps, the population can eventually either expand and grow exponentially or go extinct. **b**, The probability of replicating (blue) and the probability of dying (red) as a function of time for the same populations as in **a**. The probability of dying per unit time is fixed by temperature while the probability of replication is initially zero and increases over time as the alive cells always secrete glutathione (Fig. 5b). The probability of replicating quickly exceeds the probability of dying for high initial population densities (top row), leading to deterministic growth. For intermediate initial population densities (2nd and 3rd rows), the number of alive cells initially decreases over time as the probability of replicating continuously approaches - but stays smaller than - the probability of dying. Simultaneously, this decreasing pool of alive cells keeps secreting glutathione until, after ~300 h, the probability of replicating is very close to the probability of dying and very few alive cells are left in the population. Here, the probability of replicating either exceeds the probability of dying - leading to exponential growth - or remains smaller than the probability of dying - leading to extinction. This results in random-growth. For low initial population densities (bottom row), the probability of replicating remains well below the probability of dying. Here, the population goes extinct before the alive cells can secrete sufficient glutathione to increase the probability of replicating, leading to no growth.

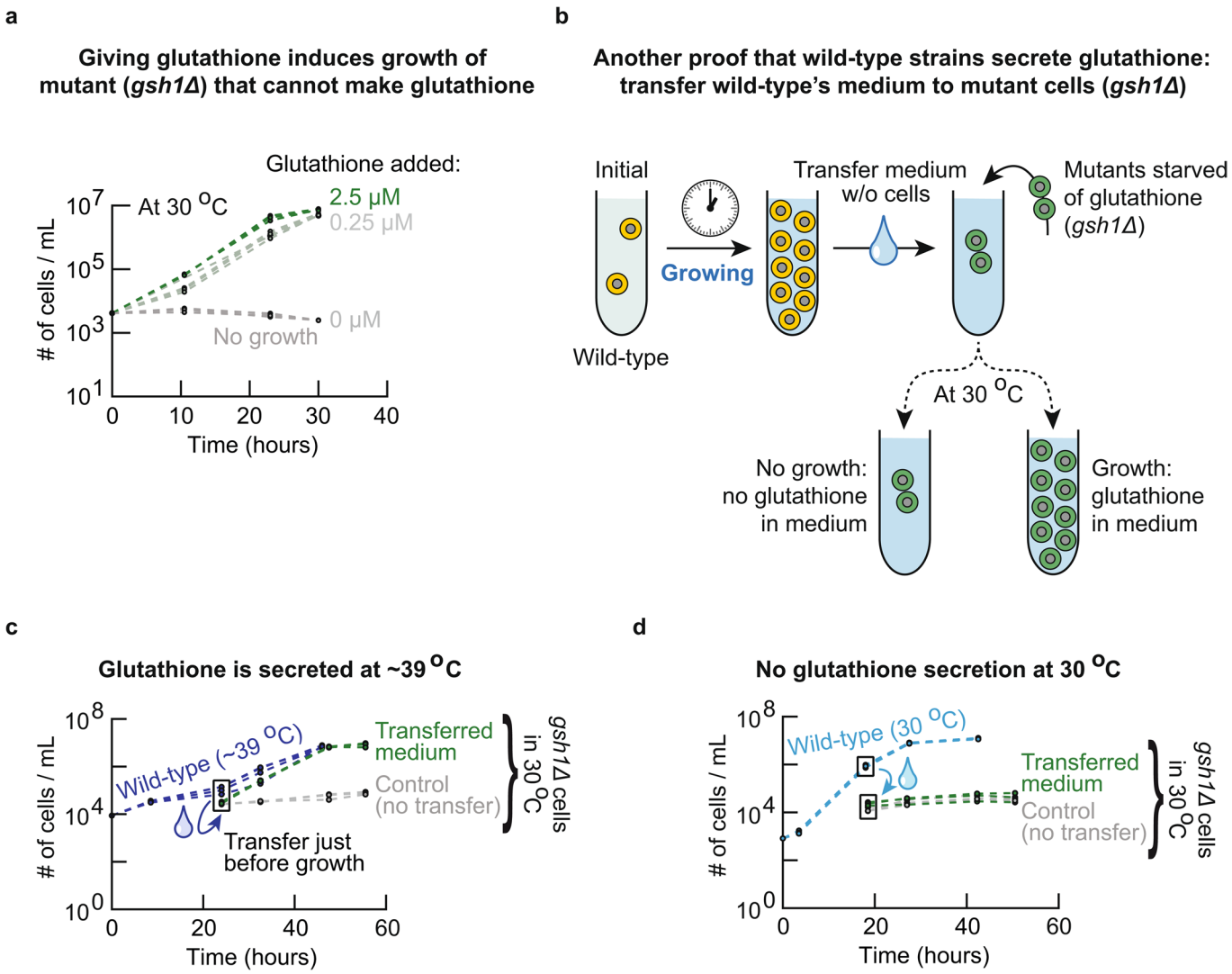

Extended Data Fig. 4 | A mutant strain that cannot synthesize glutathione detects glutathione secreted by wild-type yeasts at high temperatures (Related to Fig. 4e and Supplementary Fig. 11). a, We constructed a mutant strain that could not synthesize glutathione by knocking out, in the wild-type strain, the *GSH1* gene which is essential for glutathione biosynthesis (see "Mutant yeasts" in the Methods section). Glutathione has essential intracellular roles in yeast, so the *Δgsh1*-mutant can only grow in media that we supplement with glutathione[40]. To check this, we incubated starved the *Δgsh1*-mutant cells in SD-media to which we added 0 μM, 0.25 μM or 2.5 μM glutathione. These cells did not grow in medium without any glutathione (0 μM) but they grew in media with very small amounts of glutathione (i.e., more than 0.25 μM of extracellular glutathione). **b**, We used the *Δgsh1*-mutant strain to detect glutathione secreted by cells at high temperatures. We separated the growth media from cells grown at a fixed temperature by flowing the liquid cultures through 0.45μm-pore filters as previously described. We confirmed that there were no cells left behind in the filtered media by flowing the media through a flow cytometer. We then transplanted *Δgsh1*-mutant cells that were starved of glutathione into these filtered media at 30 °C. Subsequently, we then measured the resulting population densities over time in 30.0 °C. **c-d**, For example, we took the growth media from wild-type cells, just before growth at 39.2 °C (**c**) or during late log-phase growth at 30.0 °C (**d**). We then gave these filtered media to *Δgsh1*-cells and incubated them at 30.0 °C (green curves). As a control, we incubated populations of *Δgsh1*-cells at the same starting density in fresh media without any glutathione (grey curves). Only the media taken from cells incubated at high temperatures (39.2 °C) was able to induce growth of *Δgsh1*-cells. For all colors in each panel, there are n = 4 (**a**) or n = 3 (**c**, **d**) replicate populations. This result complements Supplementary Fig. 11, supporting our finding that wild-type cells secrete glutathione at micromolar concentrations at high temperatures (only above 36 °C).

nature research

Corresponding author(s): Hyun Youk

Last updated by author(s): Feb 29, 2020

Reporting Summary

Nature Research wishes to improve the reproducibility of the work that we publish. This form provides structure for consistency and transparency in reporting. For further information on Nature Research policies, see Authors & Referees and the Editorial Policy Checklist.

Statistics

For all statistical analyses, confirm that the following items are present in the figure legend, table legend, main text, or Methods section.

n/a	Confirmed	
☐	☒	The exact sample size (*n*) for each experimental group/condition, given as a discrete number and unit of measurement
☐	☒	A statement on whether measurements were taken from distinct samples or whether the same sample was measured repeatedly
☒	☐	The statistical test(s) used AND whether they are one- or two-sided *Only common tests should be described solely by name; describe more complex techniques in the Methods section.*
☒	☐	A description of all covariates tested
☒	☐	A description of any assumptions or corrections, such as tests of normality and adjustment for multiple comparisons
☐	☒	A full description of the statistical parameters including central tendency (e.g. means) or other basic estimates (e.g. regression coefficient) AND variation (e.g. standard deviation) or associated estimates of uncertainty (e.g. confidence intervals)
☒	☐	For null hypothesis testing, the test statistic (e.g. *F*, *t*, *r*) with confidence intervals, effect sizes, degrees of freedom and *P* value noted *Give P values as exact values whenever suitable.*
☒	☐	For Bayesian analysis, information on the choice of priors and Markov chain Monte Carlo settings
☒	☐	For hierarchical and complex designs, identification of the appropriate level for tests and full reporting of outcomes
☒	☐	Estimates of effect sizes (e.g. Cohen's *d*, Pearson's *r*), indicating how they were calculated

Our web collection on statistics for biologists contains articles on many of the points above.

Software and code

Policy information about availability of computer code

Data collection	BD FACSDiVa 8.0 & BioTek Synergy HTX
Data analysis	MATLAB R2018b, TopHat 2.1, Cufflinks 2.2

For manuscripts utilizing custom algorithms or software that are central to the research but not yet described in published literature, software must be made available to editors/reviewers. We strongly encourage code deposition in a community repository (e.g. GitHub). See the Nature Research guidelines for submitting code & software for further information.

Data

Policy information about availability of data

All manuscripts must include a data availability statement. This statement should provide the following information, where applicable:

- Accession codes, unique identifiers, or web links for publicly available datasets
- A list of figures that have associated raw data
- A description of any restrictions on data availability

The authors declare that all data supporting the findings of this study are available within the paper and its supplementary information files. The data that support the findings of this study are available from the corresponding author upon reasonable request.

Field-specific reporting

Please select the one below that is the best fit for your research. If you are not sure, read the appropriate sections before making your selection.

☒ Life sciences ☐ Behavioural & social sciences ☐ Ecological, evolutionary & environmental sciences

Life sciences study design

All studies must disclose on these points even when the disclosure is negative.

Sample size	In a given experiment, we performed measurements on n biological replicates as indicated for each figure (value of n given in each figure). Error bars report the mean with s.e.m. for these experiments.
Data exclusions	We did not exclude data.
Replication	All attempts at replication were successful and are reported as replicates (value of n reported in each figure).
Randomization	This is not relevant for our study; we performed replica experiments on different yeast colonies and on different days.
Blinding	Blinding was not necessary for our experiments; our experiments were on growth of yeasts whose results did not require statistical tests.

Reporting for specific materials, systems and methods

We require information from authors about some types of materials, experimental systems and methods used in many studies. Here, indicate whether each material, system or method listed is relevant to your study. If you are not sure if a list item applies to your research, read the appropriate section before selecting a response.

Materials & experimental systems

n/a	Involved in the study
☒	☐ Antibodies
☐	☒ Eukaryotic cell lines
☒	☐ Palaeontology
☒	☐ Animals and other organisms
☒	☐ Human research participants
☒	☐ Clinical data

Methods

n/a	Involved in the study
☒	☐ ChIP-seq
☐	☒ Flow cytometry
☒	☐ MRI-based neuroimaging

Eukaryotic cell lines

Policy information about cell lines

Cell line source(s)	EUROSCARF for the wild-type strain. We built all other strains starting from the wild-type strain as explained in "Methods".
Authentication	We checked that the strains used in this study contained all the right selection markers and the genes that we inserted at the correct locus by PCR and DNA sequencing.
Mycoplasma contamination	We used yeast cells and thus we did not test for mycoplasma contamination. We did, however, check that our cell cultures genuinely involved only yeast cells with a flow cytometer and colony assays.
Commonly misidentified lines (See ICLAC register)	No commonly misidentified cell lines were used.

Flow Cytometry

Plots

Confirm that:

☒ The axis labels state the marker and fluorochrome used (e.g. CD4-FITC).

☒ The axis scales are clearly visible. Include numbers along axes only for bottom left plot of group (a 'group' is an analysis of identical markers).

☒ All plots are contour plots with outliers or pseudocolor plots.

☒ A numerical value for number of cells or percentage (with statistics) is provided.

Methodology

Sample preparation	Yeast cells were taken from single colonies on agar pads. They were then incubated in clear, transparent minimal media (described in the methods) for the growth experiments. We then took aliquots (usually 200 uL) from the liquid culture and transferred each aliquot into a well in a 96-well plate. The High-Throughput Sampler of BD FACSCelesta injected these samples into the flow cytometer.

Instrument	BD FACSCelesta with Hight-Throughput Sampler and three lasers: 405 nm (violet), 488 nm (blue), 561 nm (yellow/green)
Software	MATLAB R2018b.
Cell population abundance	We reported all yeast cells that the flow cytometer detected; we did not exclude any yeast cells. As a control, flowing only 1x-PBS without any cells yielded no detected events in the gate settings that we used.
Gating strategy	For GFP: PMT: 485V, Filter: 530/30, Mirror: 505LP, Channel: FITC, Blue laser (488nm) For mCherry: PMT=498V, Filter 640/40, Mirror: 595LP, Channel: mCherry, Yellow-green laser - (561nm) For reporting the GFP fluorescence in Extended Data Fig. 4a and the red & white cells in Fig. 3a-c: 1) We gated the FSC & SSC to contain 67% of all cells in a density plot. 2) We gated the mCherry when taking the log-10 of intensity; the white cells were the particles in interval [1.66, 3.87] and the red cells were the particles in [4.43, 5.82]. Boundaries were chosen to clearly separate the white and red populations. The choice for FSC & SSC and mCherry gates did not change the results that we reported, as choosing another gate (or no gate) did not change the results (only scales the population-sizes proportionately).

☒ Tick this box to confirm that a figure exemplifying the gating strategy is provided in the Supplementary Information.